7-25-2016

Design of FerroElectric MEMS energy harvesting devices

Noah T. Blach
Air Force Institute of Technology

Robert A. Lake
Air Force Institute of Technology

Ronald A. Coutu Jr.
Marquette University, ronald.coutu@marquette.edu

Accepted version. 2016 IEEE National Aerospace and Electronics Conference (NAECON) and Ohio Innovation Summit (OIS) (July 25-29, 2016). DOI.
Ronald A. Coutu, Jr. was affiliated with the Air Force Institute of Technology at the time of publication.

Contents

Abstract: 2
SECTION I. Introduction 2
SECTION II. Materials 4
SECTION III. Comparable Devices 5
SECTION IV. New Approach 6
SECTION V. Conclusion 12
ACKNOWLEDGMENTS 12
References 12

Design of FerroElectric MEMS energy harvesting devices

Noah T. Blach
Electrical Engineering, Air Force Institute of Technology, Dayton, OH

Robert A. Lake
Electrical Engineering, Air Force Institute of Technology, Dayton, OH
Ronald A. Coutu
Electrical Engineering, Air Force Institute of Technology, Dayton, OH

Abstract:

Waste heat is a widely available but little used source of power. Converting a thermal gradient into electricity is conventionally done using the Seebeck effect, but devices that use this effect are naturally inefficient. An alternate approach uses microelectromechanical systems (MEMS) to generate movement and time-varying temperature from a constant temperature gradient. Ferroelectric materials can harvest electricity from moving structures and temperature variations. This concept was realized using traditional silicon microprocessing techniques. A silicon on insulator (SOI) wafer was backside Deep Reactive Ion Etched (DRIE) to form a one mm^2 by 7 micron thick silicon/silicon dioxide membrane. Lead zirconate titanate (PZT) was deposited on the membrane and acts as a ferroelectric material. Heating the bulk of the SOI substrate causes an increase in stress and upward deflection of the membrane. The membrane then enters into contact with a cold sink fixed above the substrate. Cooling of the membrane from contact with the cold sink causes actuation downwards of the membrane. The alternating heating and cooling of the PZT layer generates electricity from the pyroelectric effect. The actuation of the membrane generates stress on the PZT layer resulting in electricity from the piezoelectric effect.

SECTION I. Introduction

Heat is emitted from many energy producing devices such as combustion engines, and becomes waste heat because it is not used to generate electricity. Heat is also a byproduct of devices that consume electricity, such as computer processors. Any spatial heat gradient contains energy, which could be harvested into usable electricity by a suitable device.

The thermo-electric effect is the property of some materials to generate voltage in response to a spatial heat gradient.[1] Devices that use this effect to generate usable electrical power are called thermo electric generators (TEG), an example of which is shown in Fig. 1. TEGs are inherently low efficiency devices compared to large scale combustion engines, which typically operate near 30% of thermodynamic efficiency. TEGs typically have efficiency less than 10%, and are limited by material properties such as electrical and thermal conductivity. These devices are mainly used in spacecraft for generating electricity from the heat of nuclear decay. In the space environment, cost and efficiency are less important than weight. To make waste heat energy harvesting practical on a wider scale, a different approach is necessary.

Ferroelectric materials are those materials which have the property of maintaining a polarization after an electric field is removed.[3] These materials are also pyroelectric, and will become electrically polarized in response to a temperature change. They are also piezoelectric materials, these and generate an electrical polarization due to applied strain. The relationship between these properties is shown in Fig. 2. When a pyroelectric material is adhered to a substrate and heated, strain is generated from the stress from the different rates of expansion of the two materials. This strain then generates an electric polarization from the piezoelectric effect, and is called the secondary pyroelectric effect.

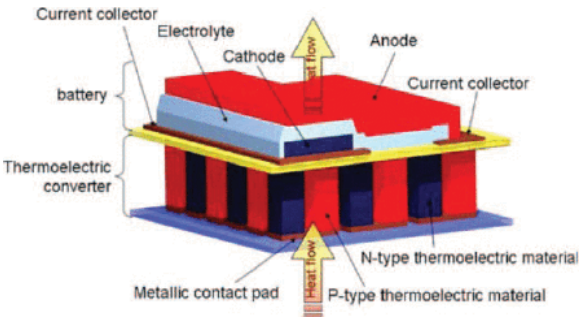

Fig. 1. This thermoelectric generator constantly generates power from a spatial heat gradient.[2]

Pyroelectricity cannot be used to directly harvest energy from a spatial gradient. This is because once heat is applied, charge will move in response to the material polarization. The material will only generate current if sequentially heated and cooled.[5] Most practical sources that generate waste heat do so constantly during operation. Since it is often impossible to cycle power to the source that generates waste heat, such as a computer processor, a mechanism must be designed to provide for mechanically moving the ferroelectric material into contact with a heat source and cold sink. While it is possible to fabricate a large mechanical system to move a bulk of ferroelectric material, research has shown that power production will increase as the dimensions of the ferroelectric device decrease.[6] When produced with microscale dimensions, energy production using pyroelectric devices is far more practical. In addition many applications of these materials, such as generating power from the heat from human skin, would require a very small device.

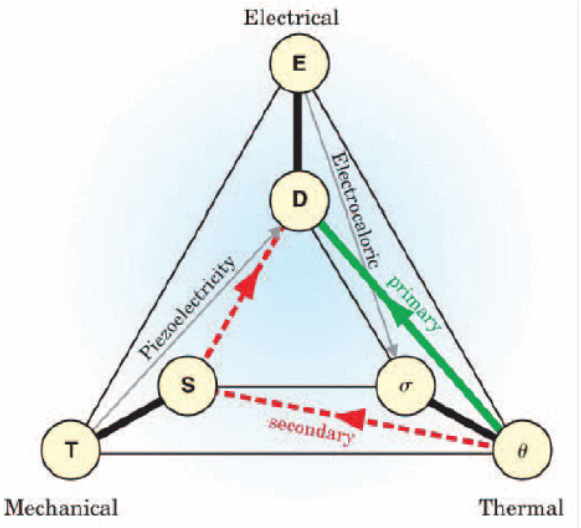

Fig. 2. Stress, heat and electric field are all interrelated in ferroelectric materials.[4]

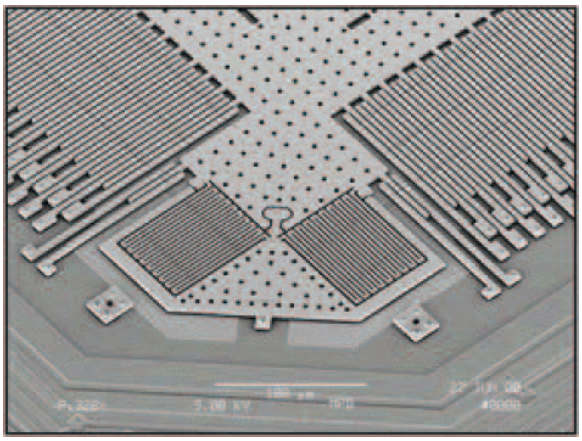

Fig. 3. Devices such as this one with features on the micrometer scale can only be fabricated with MEMS techniques.[8]

MEMS is an engineering discipline of fabricating microscale devices that grew out of the semiconductor industry.[7] The tools and methods previously used to make computer processors and silicon devices have been adapted to fabricate small mechanical systems. Optical lithography is used to define features and patterns as small as one micron in size. Deposition tools such as sputtering, evaporation, and chemical vapor deposition can be used to grow a wide variety of layers. Ion etching and wet chemical etching can be used to precisely drill down into these microlayers. MEMS technology is suited to make a microsized energy harvesting devices using ferroelectric material. Fig. 3 is an example MEMS device.

SECTION II. Materials

Materials

The predominate ferroelectric materials used in energy harvesting are polyvinylidene difluoride (PVDF) shown in Fig. 4, and lead zirconate titanate (PZT) shown in Fig. 5. PVDF is a polymer consisting of monomer units of vinylidene difluoride. When the molecular strands are oriented together, the polymer will exhibit piezoelectric properties.[11] To properly orient the PVDF units, it is common to apply a strong electric field in the presence of heat. The heat provides the energy for the molecules to reorient, and the strong electric field provides a preferential orientation. Different substituents such as TRFE (trifluoroethylene), can be added to enhance the piezoelectric properties. The most common method of depositing polymers is by spin coating. A solution of the polymer is made in a volatile solvent. The solvent is spread over the desired substrate, and then spun at high speed. The solvent will evaporate, leaving the polymer to solidify on the substrate. This method can generate an even coating of the polymer over a substrate in a variety of thicknesses.

The other common ferroelectric material in energy harvesting devices is PZT, lead zirconate titanate.[12] PZT, Pb $(\mathrm{Zr}_X\mathrm{Ti}_{1-X})\mathrm{O}_3$ is a ceramic that can crystallize in a tetragonal, rhombohedral, or cubic phase. The morphotropic phase boundary between tetragonal and rhombohedral occurs near x=.52 at room temperature. At this composition, PZT shows a large piezoelectric coefficient and a large electrical permittivity. In response to heat or stress, the ions will move in the crystal lattice generating an electric polarization. Many different substituents such as niobium can be added to tailor the properties of the ceramic material. Since PZT is a ceramic, spin coating is not possible. The most common deposition methods are sol-gel and sputtering. Sol-gel involves depositing small particles of PZT on the target, and

then sintering at high temperature to crystallize the thin film. Sputtering consists of placing a target of PZT in front of energized argon or oxygen atoms and using the kinetic transfer of momentum to eject particles onto a substrate. Annealing is then necessary to crystalize the PZT from an amorphous phase into a crystalline state.

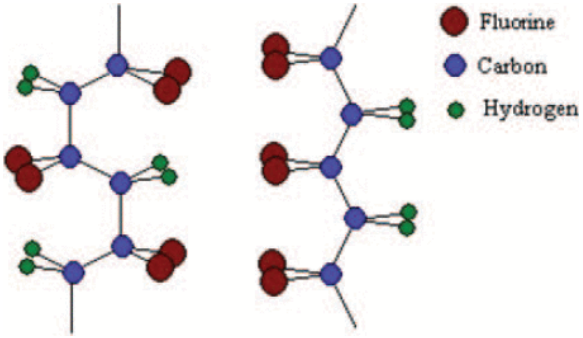

Fig. 4. PVDF molecules must be oriented and crystallized properly to show ferroelectric behavior.[9]

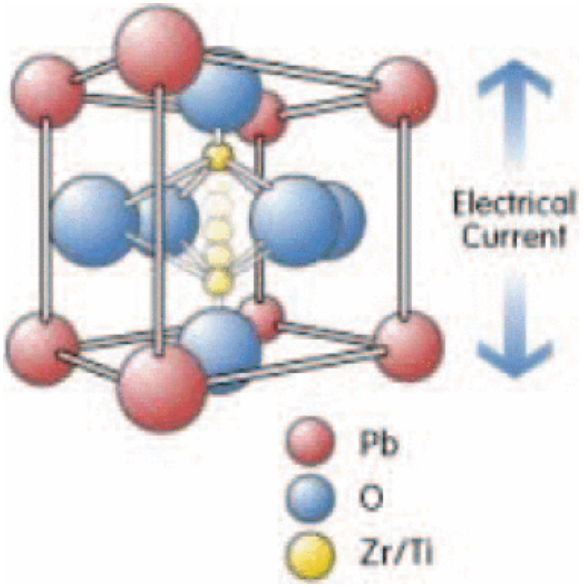

Fig. 5. As PZT is heated or stressed, the ions move creating current and power.[10]

SECTION III. Comparable Devices

One example device using MEMS and pyroelectric materials for energy harvesting consisted of adding a pyroelectric layer to a micro heat engine.[13] Ravindran *et al.*fabricated a micro heat engine shown in Fig. 6 by taking a (SOI) wafer and etching out the handle wafer. The cavity was filled with a fluid near its boiling point and then sealed. A pyroelectric layer was added. After the device was cooled, the vapor pressure would collapse the membrane inwards, forcing the device into the down state. The down state was in contact with a hot source. The hot source would heat the inside of the heat engine, causing expansion and the membrane to flip states into the up position. In the up position, the membrane would be in contact with the cold surface. The heat would leave the engine, condensing the working fluid and flipping the engine back into the down state.

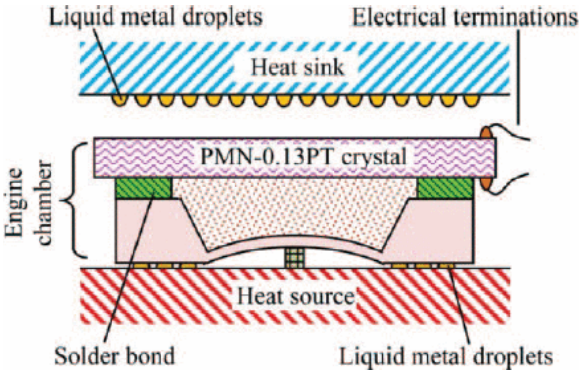

Fig. 6. This device couples a bistable motor with a ferroelectric energy harvesting layer.[14]

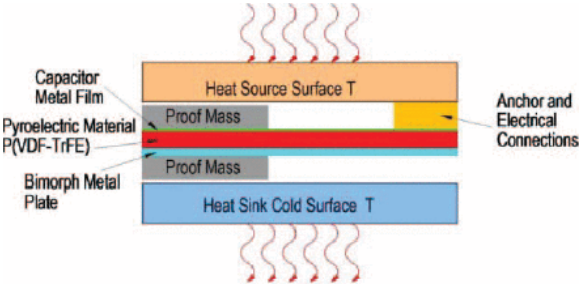

Fig. 7. At the areas of peak stress, the PZT layer should develop a potential of 3 volts.[15]

Another type of device was made by Hunter *et al.* from a cantilever structure.[15] A cantilever shown in Fig. 7 with millimeter dimensions was fabricated from silicon, and a metal layer was added on top of the cantilever. As the structure was heated and cooled, the two layers would expand at different rates due to the different coefficients of thermal expansion. This resulted in the entire structure bending upwards or downwards in response to heat. A pyroelectric layer was also added on the cantilever. Large proof masses were added over and under the tip of the cantilever. While in the up position, the heat would flow through the proof mass into the cantilever, actuating the device downwards into contact with the cold sink. While in contact with the cold sink, the opposite process would occur. The device could also be electrostatically actuated. Energy was harvested from the ferroelectric layer on the cantilever.

SECTION IV. New Approach

Instead of using a cantilever for the mechanical system, a bistable membrane will be used. These membranes are made from a SOI wafers, and consist of a bilayer of silicon and silicon dioxide with high compressive stress from the fabrication process. These membranes buckle upwards in response to stress, and respond to both heat and stress for large vertical actuations.[16,17] As heat flows into the membrane, the change in stress between the layers will result in the movement of the device into contact with a cold sink positioned above. As the membrane cooled, it will lose contact and begin heating again. This cycle would repeat indefinitely. In addition, to determine the position of the membrane without optical tools, piezoresistivity can be used to determine stress in the device.[18] This method allows for the determination of the device position even after it has been encapsulated. The wheatstone configuration was used to allow for a large increase in accuracy compared to a single resistive sensor. A heating layer made from a gold resistor can be used to test the device by injecting a specific amount of current into the device. Current running through the resistor results in heating.

Simulation results were run using CoventorWareQc, a MEMS simulation tool. The analysis shown in Fig. 8 predicts that a one micrometer PZT layer on the membrane has the potential to generate 3 volts during deflection. This voltage would be sufficient to be used for energy harvesting without using difficult low voltage techniques. The heat is predicted to diffuse out of the membrane in 10 microseconds from contact in the vertical direction, and diffuse out in the horizontal direction in one millisecond as shown in Fig. 9. This high rate of heat transfer results from the large surface contact area The dimensions of the simulated membrane are five microns of silicon, two microns silicon oxide, and one micron PZT. The membrane simulation predicts actuation in response to a change in temperature in 2 microseconds, so the device moves much faster than heat can enter or leave the device.

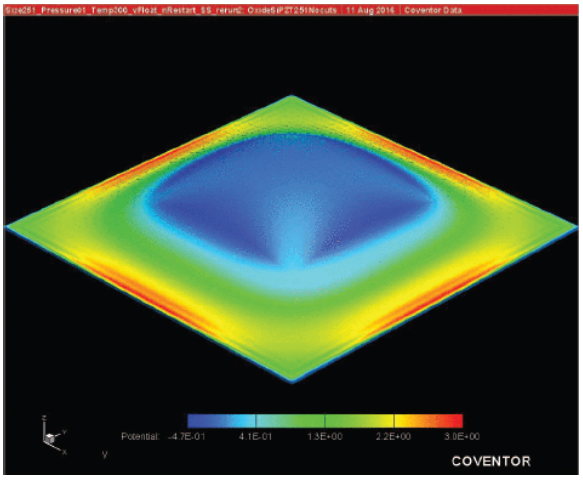

Fig. 8. At the areas of peak stress, the PZT layer should develop a potential of 3 volts.

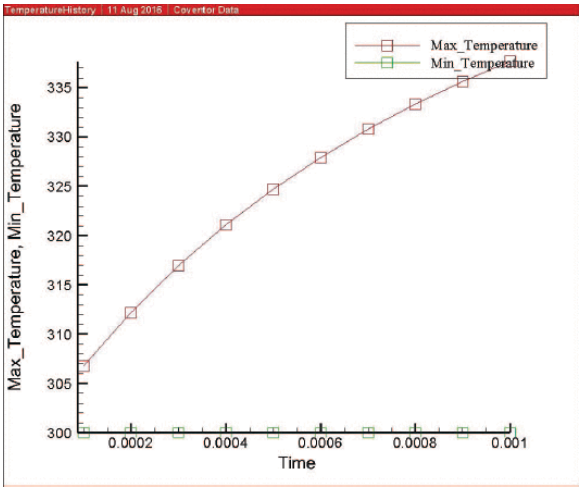

Fig. 9. Heat flows out of the device in approximately 1 millisecond

Fig. 10 through 28 show the construction of the device. Starting with an SOI wafer, a protective layer of oxide will be formed using thermal oxidation in a furnace. The oxide layer is largely resistant to the penetration of doping ions. The top oxide layer will be patterned using HF wet etching. Then a piezoresistive sensor will be fabricated by diffusing phosphorous into the wafer using the oxide as a mask. The oxide will be removed using HF etching. Next, a gold layer serving both as electrical contacts to the piezoresistive sensors and as a heating layer will be deposited via evaporation. The gold trace across the membrane will dissipate electrical heat as energy. The gold layer will be patterned using a

liftoff technique. An insulating layer of silicon nitride will be deposited by plasma enhanced chemical vapor deposition (PECVD) and patterned using reactive ion etching. This layer will electrically separate the gold heating layer and the ferroelectric energy layer. Afterwords, the lower platinum electrode will be deposited by sputtering, using 10 nanometers of titanium for adhesion. PZT will be sputtered across the entire wafer, and patterned using reactive ion etching with boron trichloride. The PZT will be thermally annealed for 5 minutes at 650 Celcius. The upper electrode will be formed from evaporated gold and patterned using a liftoff technique. Lastly, the back of the sample will be etched by DRIE, and the intrinsic stress of the silicon and silicon oxide layers will cause the structure to bend into a membrane structure. A negative SU-8 photoresist will define the DRIE etching areas. The SU-8 photoresist will remain on the device after the DRIE as a permanent feature.

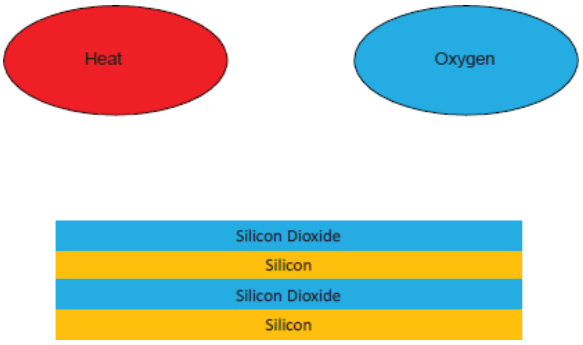

Fig. 10. Heat and oxygen cause the growth of a 120 nanometer thermal oxide layer on the surface of the SOI wafer.

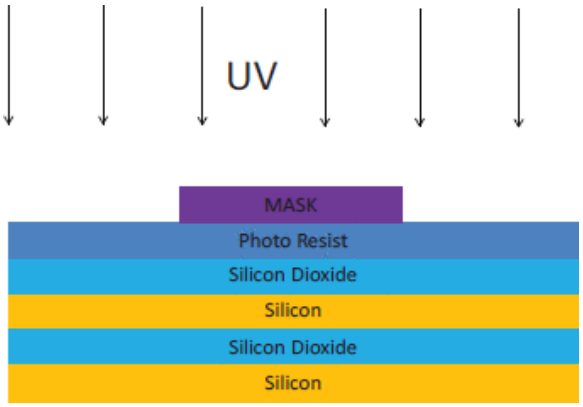

Fig. 11. Photoresist is applied to the wafer, exposed and developed.

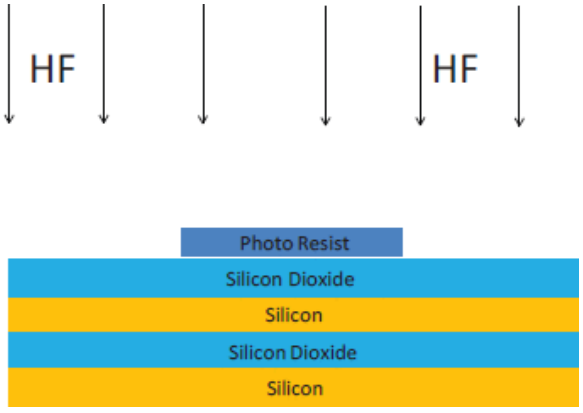

Fig. 12. HF acid is used to etch a pattern in the thermal oxide.

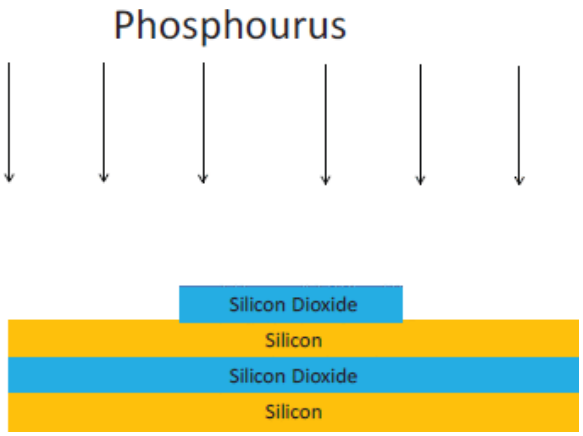

Fig. 13. After the photoresist is removed, phosphorous is diffused into the wafer by placing a dopant source adjacent to the sample at 1000 degrees C.

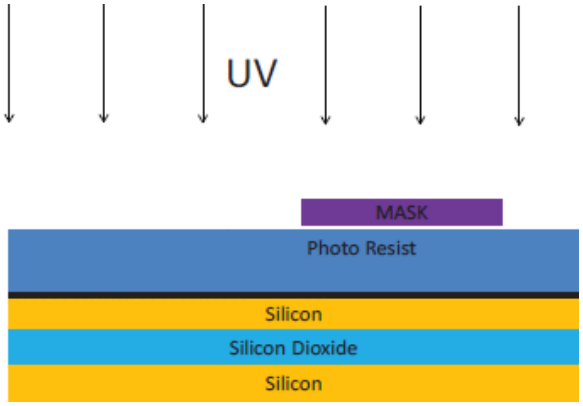

Fig. 14. After the remaining oxide is removed by an HF bath, another layer of photoresist is applied, exposed and patterned.

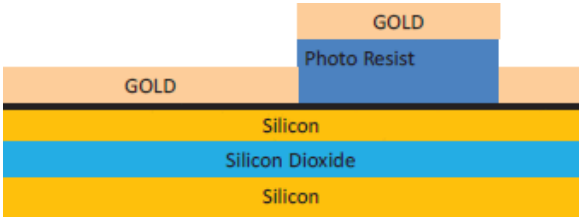

Fig. 15. 150 nanometers of gold and 20 nanometers of titanium for adhesion are thermally evaporated across the sample.

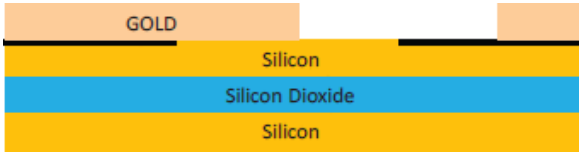

Fig. 16. A liftoff procedure removed the gold that adhered to the photoresist, and the remaining resist is removed.

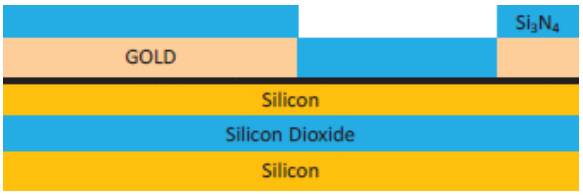

Fig. 17. A layer of silicon nitride is grown using PECVD for insulating the just deposited gold layer and the electrode layers above.

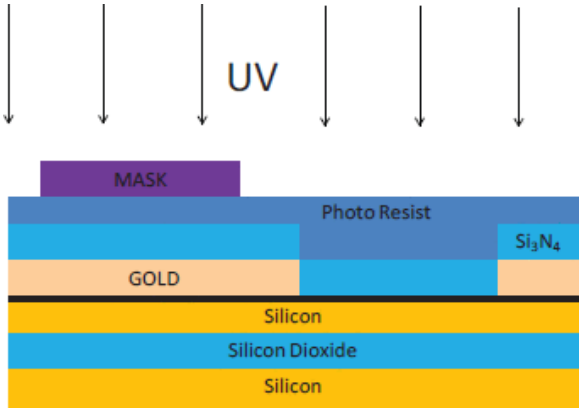

Fig. 18. A layer of photoresist is applied, exposed and patterned.

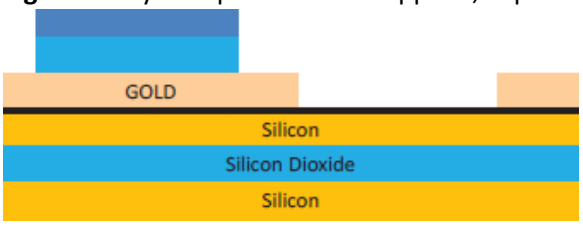

Fig. 19. The pattern is transferred into the nitride by reactive ion etching

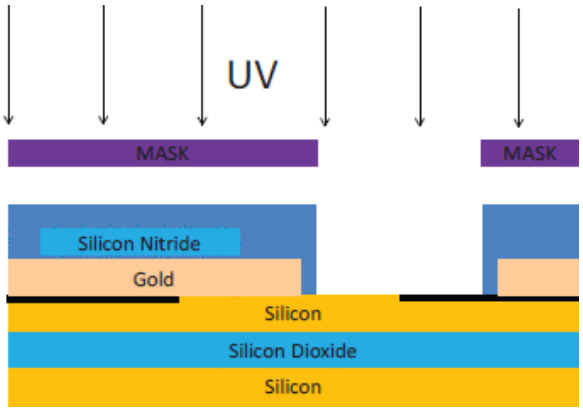

Fig. 21. Platinum is sputtered onto the sample, using titanium as an adhesion layer.

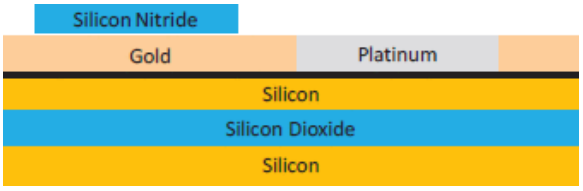

Fig. 22. The liftoff procedure completes the pattern definition of the bottom platinum electrode.

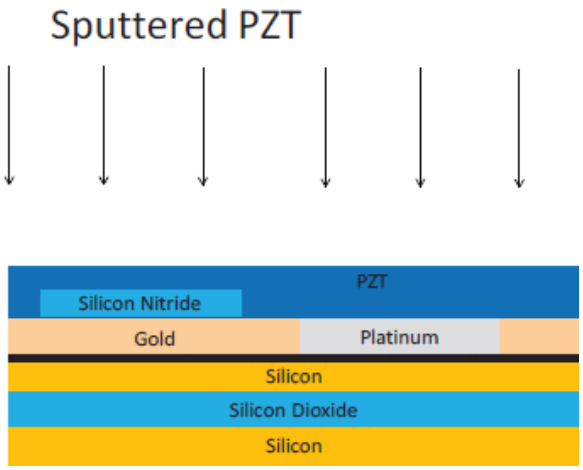

Fig. 23. 1 micrometer of PZT is sputtered across the entire surface.

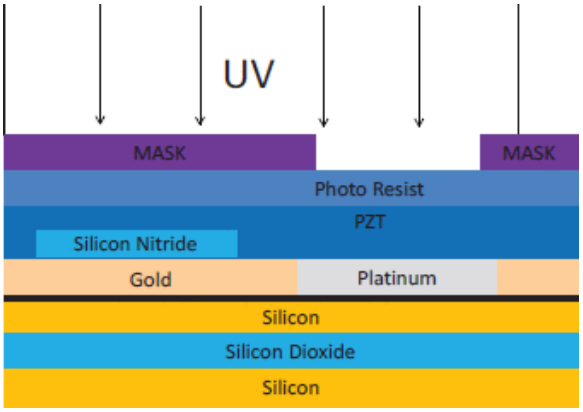

Fig. 24. Photoresist is patterned to prepare for PZT etching

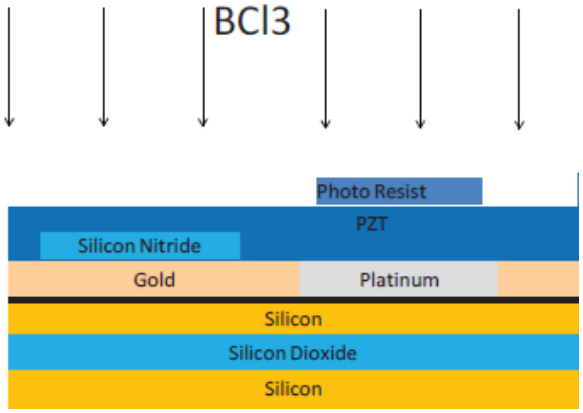

Fig. 25. The PZT is reactive ion etched by boron trichloride

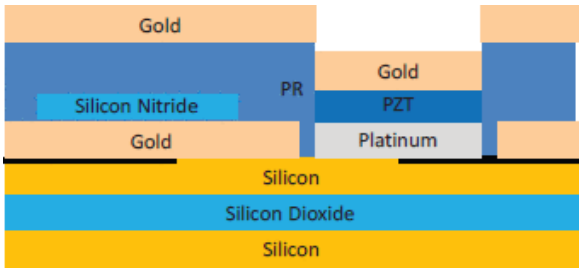

Fig. 26. The liftoff sequence is repeated again for the deposition of a top gold electrode.

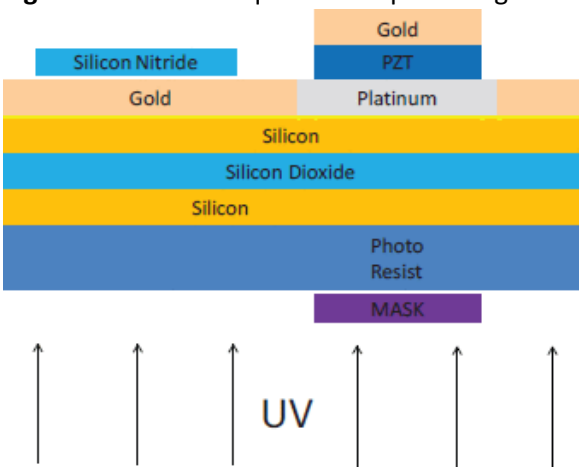

Fig. 27. A negative photoresist is used to pattern the bottom side of the wafer for DRIE.

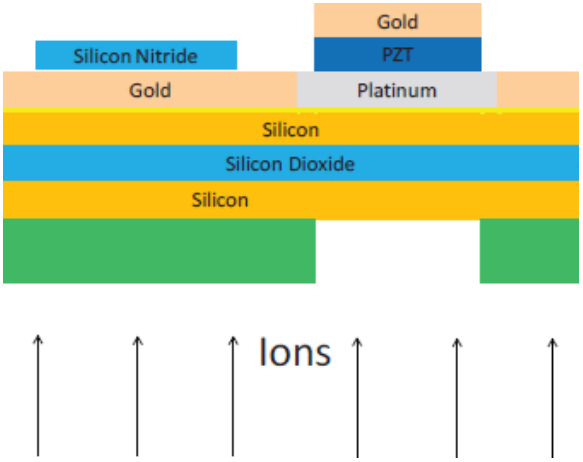

Fig. 28. The hardened negative photoresist provides a mask for DRIE etching of the wafer.

SECTION V. Conclusion

Using this design, it will be possible to construct a MEMS energy harvesting device that responds at high speeds. The device will be constructed entirely using whole wafer techniques. The volume, at near one cubic millimeter, will be small enough to be effectively deployed anywhere. The only limits on shrinking this device are the dimensions of the SOI wafer. SOI wafers are available at 200 nanometers thick device layer, which would correspond to a device 40 microns across.

ACKNOWLEDGMENTS

The authors wish to thank Adam Fritzsche, Rich Johnston, Major Tod Laurvick and Major Jim Sattler for their device fabrication and test support.

References

1. M. Hamid, D. A. Shnawah Elsheikh, M. F. M. Sabri, S. B. M. Said, M. Haji Hassan, M. B. Ali Bashir, M. Mohamad, "A review on thermoelectric renewable energy: Principle parameters that affect their performance", *Renewable and Sustainable Energy Reviews*, vol. 30, pp. 337-355, 2014.

2. J. Carmo, L. Gonçalves, J. Correia, "Thermoelectric micro converter for energy harvesting systems", *IEEE Transactions on Industrial Electronics*, vol. 57, no. 3, pp. 861, 2010.
3. K. Uchino, K. Uchino, "1 — The development of piezoelectric materials and the new perspective" in Advanced Piezoelectric Materials, Woodhead Publishing, pp. 1-85, 2010.
4. S. B. Lang, "Pyroelectricity: From Ancient Changes in the net dipole moment of certain materials form", *Physics Today*, pp. 31-36, August 2005.
5. P. Mane, J. Xie, K. K. Leang, K. Mossi, "Cyclic energy harvesting from pyroelectric materials", *IEEE Transactions on Ultrasonics Ferroelectries and Frequency Control*, vol. 58, no. 1, pp. 10-17, 2011.
6. O. Puscasu, S. Monfray, F. Boeuf, G. Savelli, F. Gaillard, D. Guyomar, T. Skotnicki, "Scale laws for enhanced power for MEMS based heat energy harvesting", *Silicon Nanoelectronics Workshop*, pp. 1-2, 2012.
7. M. J. Madou, Manufacturing Techniques for Microfabrication and Nanotechnology, Taylor & Francis, 2011, [online] Available: https://books.google.com/books?id=CKy5zj94xqQC.
8. "No Title", [online] Available: http://fadikhalil.perso.sfr.fr/MEMS.html.
9. "No Title", [online] Available: http://www.plasticseurope.org/what-is-plastic/types-of-plastics-11148/engineering-plastics/pvdf.aspx.
10. "No Title", [online] Available: http://electronicstructure.wikidot.com/first-principles-study-of-piezoelectricity-in-pzt.
11. H. Nguyen, A. Navid, L. Pilon, "Pyroelectric energy converter using co-polymer P(VDF-TrFE) and Olsen cycle for waste heat energy harvesting", *Applied Thermal Engineering*, vol. 30, no. 14–15, pp. 2127-2137, 2010.
12. K. Kanda, I. Kanno, H. Kotera, K. Wasa, "Simple fabrication of metal-based piezoelectric MEMS by direct deposition of Pb(Zr Ti) O3 thin films on titanium substrates", *Journal of Microelectromechanical Systems*, vol. 18, no. 3, pp. 610-615, 2009.
13. S. K. T. Ravindran, M. Kroener, P. Woias, "A bimetallic micro heat engine for pyroelectric energy conversion", *Procedia Engineering*, vol. 47, no. 1, pp. 33-36, 2012.
14. S. K. T. Ravindran, T. Huesgen, M. Kroener, P. Woias, "A self-sustaining micro thermomechanic-pyroelectric generator", *Applied Physics Letters*, vol. 99, no. 10, pp. 104102, 2011.
15. S. R. Hunter, N. V. Lavrik, T. Bannuru, S. Mostafa, S. Rajic, P. G. Datskos, "Development of MEMS based pyroelectric thermal energy harvesters", *Energy harvesting and storage*, vol. 8035, pp. 80 350V-80 350V-12, March 2011.
16. D. Popescu, T. Lammerink, M. Elwenspoek, "Buckled membranes for microstructures", *Proceedings IEEE Micro Electro Mechanical Systems An Investigation of Micro Structures Sensors Actuators Machines and Robotic Systems*, pp. 188-192, 1994.
17. R. A. Lake, K. K. Ziegler, R. A. Coutu, "Thermal tuning of MEMS buckled membrane actuator stiffness", *Procedia Engineering*, vol. 87, pp. 1382-1385, 2014.
18. H. C. Chang, H. S. Hsieh, S. C. Lo, C. F. Hu, W. Fang, "Piezoresistive pressure sensor with Ladder shape design of piezoresistor", *Proceedings of IEEE Sensors*, vol. 1, 2012.